Serb. Astron. J. № 199 (2019), 55 - 64 **UDC 524.7 : 521.96 ICRF, Gaia CRF**
DOI: https://doi.org/10.2298/SAJ1999055J Original scientific paper

OPTICAL VARIABILITY OF SOME QUASARS IMPORTANT TO ICRF-GAIA CRF LINK

Miljana D. Jovanović

Astronomical Observatory, Volgina 7, 11060 Belgrade 38, Serbia
E–mail: *miljana@aob.rs*

(Received: July 3, 2019; Accepted: September 3, 2019)

SUMMARY: The Gaia optical observations started a few years ago. As a result, the Gaia Celestial Reference Frame (Gaia CRF) should replace the International CRF (ICRF). This could be done via extragalactic radio sources (mostly quasars - QSOs) visible in optical domain. During about 2.5 years (for the period July 2016 – April 2019) of our original observations of some QSOs outside ICRF list we collected observations in the V and R bands for five objects and their 30 comparison stars. Photometry stability of these objects is of importance for astrometry and the mentioned link. Because of it we did investigation of brightness variability of objects and their suitable comparison stars, and the F–test was performed. As a result, only the brightness of one object (1556+335) does not show variability. Other four objects were examined to determine the quasiperiods of their light curves using the method of Least Squares: 1535+231 (3.1 years in V, and 1.7 and 5.2 years in R filter), 1607+604 (2.7 years in V, and 1.3 and 2.3 years in R), 1722+119 (1.3 and 2.7 years in V, and 1.3 and 5.3 years in R), and 1741+597 (6.5 years in V, and 1.3 and 4.0 years in R). After a similar analysis of variability of comparison stars, the conclusion is that all of them are useful for differential photometry. Also, we provide our finding charts for these objects with suitable comparison stars.

Key words. Galaxies: active – Methods: – data analysis – Techniques: photometric

1. INTRODUCTION

Since 1st January 2019 the fundamental celestial reference frame recognised by the International Astronomical Union has been the International Celestial Reference Frame 3 - ICRF3 (http://hpiers.obspm.fr/icrs-pc/newwww/icrf/icrf3-ReadMe.txt) as a follow-up on the initial realization of ICRF and its successor adopted in 2009 (Fey et al. 2015). ICRF3 contains coordinates of 4536 extragalactic radio sources in J2000.0, determined by using Very Long Baseline Interferometry - VLBI; out of which 303 uniformly distributed in the sky are identified as defining sources and, as such, serve to define the axes of the frame.

The Gaia satellite of the European Space Agency was launched in December 2013; Gaia is the acronym for Global Astrometric Interferometer for Astrophysics. The actual Gaia Data Realize 2 (Gaia DR2) has been made available publicly since April 2018 (Gaia Collaboration et al. 2018). Gaia DR2 contains astrometric parameters (positions, parallaxes, and proper motions) for more than 1.3 billion sources (of which 550 000 are QSOs – quasars). A new highly-accurate optical Gaia Celestial Reference Frame (Gaia CRF) will be one of the most important results of the Gaia mission, and at the accuracy level of ICRF. For continuity the orientation of the Gaia CRF axes (fixed with respect to distant extragalactic objects) should coincide with ICRF as much as po-

ssible. The link between Gaia CRF and ICRF will be established by using Gaia observations in optical domain of compact extragalactic ICRF objects with accurate radio positions, but only about 70 ICRF sources are suitable. Because of that, 105 extragalactic radio sources (out of the ICRF list) were observed with a VLBI array and 47 of them with high astrometric quality have been identified as potential candidates for the link (Bourda et al. 2011). Our observations of these candidate sources started in July 2016. These sources are Active Galactic Nuclei (AGNs), most of them are the QSO type (30 sources), the others are BL Lacertae – BL Lac (15) and Seyfert galaxies type 1 – Sy 1 (2).

An AGN represents a life phase of a galaxy. The term active refers to existence of energetic phenomena in the galactic center, nucleus, which cannot be attributed directly to stars. Presence of variations in optical and radio bands has led to suggestions that there exists a massive black hole in the center of AGN. These variations on time scales of less than a day to years are very important to understand their physical properties. Time scale variability is divided into three classes: those of less than a day are Intra–Day Variabilities – IDV, those within the range of a few days to a few months are Short Term Variability – STV, and those from a few months to several years are Long Term Variability – LTV (Gupta 2014). There are several papers on correlation between the brightness variability and astrometric positions of QSOs in some cases (Taris et al. 2011, 2016, Popović et al. 2012). For the link between Gaia CRF and ICRF the sources with more stable brightness are preferred, and it is necessary to monitor their brightness variability over a longer period of time. Some results of STV of the mentioned objects are presented in Taris et al. (2018).

The subject of this paper is investigation of the brightness variability of five AGNs which have been observed for more than 2.5 years. Two of them are the type QSOs (1535+231 and 1556+335) and three BL Lac (1607+604, 1722+119, and 1741+597). The object properties are listed in Table 1: the coordinates are taken from SDSS DR14, the redshift is from the NASA/IPAC Extragalactic Database – NED (https://ned.ipac.caltech.edu/), and the type is from SIMBAD Astronomical Database.

2. OBSERVATIONS AND DATA REDUCTION

The observations were made with three different telescopes using six different cameras (see Table 2). The Astronomical Station Vidojevica (ASV) 60 cm Cassegrain and the ASV 1.4 m Ritchey-Chrétien telescope are located at Astronomical Station Vidojevica of the Astronomical Observatory of Belgrade. For both telescopes the longitude and the latitude are $\lambda = 21\overset{\circ}{.}5$ East and $\varphi = 43\overset{\circ}{.}1$ North but the altitudes are slightly different: ASV 60 cm at 1140 m, and ASV 1.4 m at 1150 m above the sea level. Most frequently, two CCD images per filter (V and R) have been obtained. The CCD images were reduced by subtracting bias and dark and then divided by the flat field. All frames were corrected for bad pixels and cosmic rays. The reduction (and corrections) were done by using Image Reduction and Analysis Facility - the IRAF scripting language (ascl:9911.002) (Tody 1986, 1993).

The Rozhen 2m-telescope, which also has Ritchey-Chrétien optical design, is located at the National Astronomical Observatory (NAO) Rozhen of the Bulgarian Academy of Science (BAS) in Bulgaria ($\lambda = 24\overset{\circ}{.}7$ East, $\varphi = 41\overset{\circ}{.}7$ North, altitude 1730 m). The reduction of its frames was similar to that in the case of the ASV telescopes.

Table 1. Main properties of the objects.

Object	$\alpha_{\mathrm{J2000.0}}(^\circ)$	$\delta_{\mathrm{J2000.0}}(^\circ)$	z	Type	Observation date (mmddyyyy)		No. of observations per filter
					start	finish	V, R
1535+231	234.31041	23.01126	0.462524	QSO	07022016	04072019	17, 21
1556+335	239.72993	33.38851	1.653476	QSO	07022016	10052018	17, 24
1607+604	242.08560	60.30783	0.178000	BL Lac	07022016	11132018	20, 24
1722+119	261.26810	11.87096	0.018000	BL Lac	07022016	03062019	21, 23
1741+597	265.63334	59.75186	0.400000	BL Lac	07042016	03062019	31, 37

Table 2. Telescopes and cameras.

Telescope focal length	CCD Camera	CCD resolution	Pixel size (μm)	Pixel scale (arcsec pix^{-1})	Field of view (arcmin)
ASV 60cm	Apogee Alta U42	2048x2048	13.5x13.5	0.466	15.8x15.8
$F = 600$cm	SBIG ST10 XME	2184x1472	6.8x6.8	0.230	8.4x5.7
	Apogee Alta E47	1024x1024	13.0x13.0	0.450	7.6x7.6
ASV 1.4m	Apogee Alta U42	2048x2048	13.5x13.5	0.243	8.3x8.3
$F = 1142$cm	Andor iKon-L	2048x2048	13.5x13.5	0.244	8.3x8.3
Rozhen 2m	Andor iKon-L	2048x2048	13.5x13.5	0.176	6.0x6.0
$F = 1577$cm	VersArray 1300B	1340x1300	20.0x20.0	0.261	5.6x5.6

Table 3. Coordinates and BVRI magnitudes with standard errors of comparison and control stars for objects 1535+231, 1556+335, 1607+604, 1722+119, and 1741+597.

Object						
No.	$\alpha_{J2000.0}(^\circ)$	$\delta_{J2000.0}(^\circ)$	$B \pm \sigma_{\rm B}$(mag)	$V \pm \sigma_{\rm V}$(mag)	$R \pm \sigma_{\rm R}$(mag)	$I \pm \sigma_{\rm I}$(mag)
1535+231						
2	234.31491	23.01831	18.119 ± 0.049	17.200 ± 0.031	16.658 ± 0.038	16.127 ± 0.072
3	234.30004	23.02486	16.580 ± 0.040	15.983 ± 0.030	15.633 ± 0.031	15.287 ± 0.051
4	234.25178	23.01917	16.849 ± 0.037	16.232 ± 0.024	15.867 ± 0.029	15.497 ± 0.052
7	234.29312	22.96096	17.302 ± 0.044	16.470 ± 0.027	15.973 ± 0.036	15.465 ± 0.069
8	234.35917	23.01592	17.054 ± 0.060	15.860 ± 0.035	15.149 ± 0.050	14.445 ± 0.098
1556+335						
2	239.71950	33.39110	18.141 ± 0.045	17.336 ± 0.030	16.850 ± 0.038	16.341 ± 0.069
3	239.69035	33.40959	16.853 ± 0.036	16.381 ± 0.027	16.095 ± 0.030	15.773 ± 0.048
5	239.76798	33.38778	16.864 ± 0.040	16.271 ± 0.030	15.916 ± 0.031	15.539 ± 0.055
6	239.74562	33.39003	16.823 ± 0.041	16.198 ± 0.030	15.825 ± 0.031	15.438 ± 0.056
7	239.74317	33.37370	16.161 ± 0.040	15.552 ± 0.030	15.188 ± 0.031	14.808 ± 0.055
8	239.73398	33.37219	17.132 ± 0.069	15.743 ± 0.040	14.897 ± 0.064	14.008 ± 0.130
1607+604						
2	242.02882	60.28951	17.836 ± 0.043	17.068 ± 0.027	16.619 ± 0.031	16.190 ± 0.058
3	242.02526	60.31162	17.624 ± 0.041	16.864 ± 0.025	16.423 ± 0.032	16.009 ± 0.057
4	241.97352	60.35552	15.909 ± 0.040	15.195 ± 0.025	14.781 ± 0.031	14.388 ± 0.055
5	242.09638	60.34816	16.774 ± 0.056	15.630 ± 0.031	14.965 ± 0.044	14.351 ± 0.084
7	242.16854	60.37746	17.512 ± 0.038	16.856 ± 0.024	16.467 ± 0.031	16.069 ± 0.055
1722+119						
C2	261.27167	11.86997	14.203 ± 0.009	13.173 ±0.005	12.570 ±0.006	12.060 ± 0.009
C3	261.24375	11.86636	14.919 ± 0.022	14.078 ±0.012	13.600 ±0.008	13.148 ± 0.016
1	261.31208	11.89125	14.564 ± 0.012	13.445 ±0.009	12.848 ±0.010	12.272 ± 0.012
2	261.30458	11.86519	15.088 ± 0.013	14.823 ±0.008	14.691 ±0.012	14.526 ± 0.025
5	261.25667	11.91311	16.780 ± 0.033	15.873 ±0.010	15.385 ±0.016	14.927 ± 0.031
9	261.23333	11.87083	16.628 ± 0.029	15.809 ±0.008	15.332 ±0.014	14.867 ± 0.029
10	261.23875	11.87083	16.684 ± 0.035	16.142 ±0.011	15.699 ±0.019	15.272 ± 0.041
C4	261.28958	11.85344	16.563 ± 0.027	15.665 ±0.009	15.164 ±0.013	14.713 ± 0.025
1741+597						
2	265.62329	59.75176	16.175 ± 0.039	15.565 ± 0.029	15.204 ± 0.054	14.837 ± 0.054
3	265.57081	59.75387	17.288 ± 0.039	16.673 ± 0.029	16.314 ± 0.053	15.962 ± 0.053
4	265.68412	59.76861	17.409 ± 0.054	16.376 ± 0.034	15.795 ± 0.067	15.313 ± 0.067
5	265.61457	59.79547	16.953 ± 0.045	16.154 ± 0.031	15.704 ± 0.056	15.320 ± 0.056
6	265.68288	59.71901	16.861 ± 0.047	16.126 ± 0.038	15.684 ± 0.064	15.223 ± 0.064
7	265.59766	59.71686	17.479 ± 0.050	16.633 ± 0.039	16.124 ± 0.074	15.594 ± 0.074

3. PHOTOMETRY

The brightness of the target objects was determined by differential photometry, i.e., by comparing the brightness of an object to brightness of comparison stars. Two stars were chosen as comparison ones. Their brightness is similar to that of the object and they are located in its vicinity. In addition, a few control stars were selected and their photometry was performed in the same way as for the object. For this purpose the MaxIm DL software was used with the aperture radius of about 6 arcsec. The annulus radii (for determination of the sky background) were selected to avoid any forms of light contamination.

The comparison and control stars were chosen from the Sloan Digital Sky Survey Data Release 14 (SDSS DR14) catalogue (Abolfathi et al. 2018). The field of 1722+119 objects was not covered by SDSS, because the sky coverage of SDSS DR14 is about one-third of the entire celestial sphere. The selection criteria for stars were the following: not to be variable, not too far from the object, avoiding both too bright and too faint stars, not very blue or red, etc. The PSF ugriz (the point spread function u, g, r, i, and z) magnitudes for the comparison and control stars were selected from the catalogue. The transformation from the PSF ugriz magnitudes to the Johnson-Cousins BVRI (B, V, R, and I) ones was performed using equations (Chonis and Gaskel 2008):

$$B = g + (0.327 \pm 0.047)(g - r) + (0.216 \pm 0.027), \quad (1)$$

$$V = g - (0.587 \pm 0.022)(g-r) - (0.011 \pm 0.013), \quad (2)$$

$$R = r - (0.272 \pm 0.092)(r-i) - (0.159 \pm 0.022), \quad (3)$$

$$I = i - (0.337 \pm 0.191)(r-i) - (0.370 \pm 0.041), \quad (4)$$

where $14.5 < g, r, i < 19.5$, $0.08 < r - i < 0.5$ and $0.2 < g - r < 1.4$.

In the case of 1722+119 the comparison and control stars were chosen from Doroshenko et al. (2014).

The BVRI magnitudes, obtained using Eqs. (1) – (4) for stars from SDSS DR14, and those from Doroshenko et al. (2014), along with their coordinates, are listed in Table 3.

Figs. 1 – 5 represent charts of the fields of objects, created using the CCD images taken with the ASV 60 cm and CCD camera Apogee Alta U42. For each figure, the number 1 refers to the object from the caption, except for 1722+119 indicated by the cross. The other numbers refer to comparison and control stars.

The average magnitude of quasar 1535+231 is 18.322 (standard deviation, σ=0.160) in V, and 18.050 (σ=0.180) in R band during our observational period of 1008 days (∼2.76 years). The finding chart of this object with the comparison (A and B in Table 4) and control stars is presented in Fig. 1. The obtained extremal magnitudes of the object (maximum and minimum values) during that period are: 18.132 and 18.654 in the V filter, 17.796 and 18.451 in the R filter, respectively.

Quasar 1556+335 was observed during 825 days (∼2.26 years). Photometrically, this object is the most stable one, its magnitudes are close to the average value: 17.491 (σ=0.045) in V and 17.017 (σ=0.041) in R. In Fig. 2 comparison and control stars around object are presented.

The object 1607+604 BL Lac was observed during 864 days (∼2.36 years). The average magnitude is: 17.461 with σ=0.113 in V, and 17.038 with σ=0.087 in R. This object with its comparison and control stars is presented in Fig. 3. The obtained values for the maximum and minimum brightness are: 17.304 and 17.617 in V, 16.886 and 17.148 in R, respectively.

The object 1722+119 BL Lac was observed for 977 days (∼2.67 years); see Fig. 4 for the finding chart. The average magnitude is: 15.279 (σ=0.268) in V, and 14.788 (σ=0.285) in R. During the monitoring, the obtained V and R magnitudes of the object show a remarkable variability of about 1.2 magnitudes (possible quasiperiodicity). Because of the remarkable variability the standard deviations in V and R are bigger than for the others objects. The extremal magnitudes are: 14.888 and 16.080 in V, 14.372 and 15.634 in R. In Taris et al. (2018) it is presented a period of 35 days of brightness variability for optical G magnitude. Brightness variability was analysed also in X-ray from data covering more than 12 years (Rani et al. 2009). In that paper the period of about one year was explained as observational artifact.

The object 1741+597 is also BL Lac, and was observed during 975 days (∼2.67 years). Its average magnitude is: 18.038 (σ=0.218) in V and 17.623 (σ=0.261) in R. The magnitude range is from 17.588 to 18.470 in V, and 17.106 to 18.171 in R. The brightness of this object changed by almost 1 magnitude in both filters. In Fig. 5 the finding chart of object and its comparison and control stars is presented.

The standard deviations of comparison and control stars of all objects are on the level of 0.01 (see Table 4), which is in line with groundbased relative photometry.

Table 4. Average magnitudes (V and R) with standard errors of objects 1535+231, 1556+335, 1607+604, 1722+119, 1741+597, their comparison and control stars; period July 2016 - April 2019.

Object No.	$V \pm \sigma_V$(mag)	$R \pm \sigma_R$(mag)
1535+231	18.322 ±0.160	18.050 ±0.180
2 (A)	17.212 ±0.026	16.696 ±0.038
3	16.003 ±0.026	15.660 ±0.031
4 (B)	16.227 ±0.010	15.850 ±0.018
7	16.448 ±0.029	15.956 ±0.023
8	15.834 ±0.019	15.140 ±0.028
1556+335	17.491 ±0.045	17.017 ±0.041
2 (A)	17.343 ±0.033	16.898 ±0.032
3 (B)	16.378 ±0.014	16.072 ±0.015
5	16.288 ±0.027	15.934 ±0.023
6	16.224 ±0.024	15.878 ±0.021
7	15.567 ±0.024	15.224 ±0.018
8	15.746 ±0.040	14.966 ±0.017
1607+604	17.461 ±0.113	17.038 ±0.087
2	17.075 ±0.041	16.621 ±0.041
3 (A)	16.899 ±0.033	16.464 ±0.028
4	15.172 ±0.050	14.736 ±0.033
5 (B)	15.619 ±0.010	14.955 ±0.007
7	16.837 ±0.034	16.393 ±0.039
1722+119	15.279 ±0.268	14.788 ±0.285
C2	13.177 ±0.019	12.631 ±0.028
C3	14.087 ±0.024	13.632 ±0.017
1	13.438 ±0.022	12.856 ±0.025
2 (A)	14.830 ±0.008	14.688 ±0.005
5	15.863 ±0.051	15.375 ±0.022
9	15.802 ±0.024	15.339 ±0.020
10	16.141 ±0.026	15.713 ±0.022
C4 (B)	15.651 ±0.017	15.169 ±0.007
1741+597	18.038 ±0.218	17.623 ±0.261
2	15.622 ±0.032	15.295 ±0.041
3 (A)	16.679 ±0.014	16.332 ±0.016
4	16.406 ±0.030	15.840 ±0.025
5	16.188 ±0.042	15.752 ±0.025
6	16.137 ±0.024	15.696 ±0.023
7 (B)	16.628 ±0.014	16.110 ±0.013

Note. (A), (B) refer to comparison stars.

In Table 4 the average values and their standard deviations in V and R bands of objects and stars for the period July 2016 – April 2019 are presented.

As an example, light curves of object 1741+597 (black line), its comparison (3, and 7 - red) and control stars (2, 4, 5, and 6 - blue lines) are given in Fig. 6. This object, with 37 observation nights, is the most observed object in R filter. Variability of object is evident from light curve, especially in comparison with the light curves of comparison and control stars. It is confirmed using F–test.

4. ANALYSIS METHODS

The 3–σ rule was applied to reject some data. In the case of normal distribution, almost all of the data (99.7%) lie within three standard deviations of the average value. According to this, two points of the object 1722+119 were rejected: at 22$^{\rm nd}$, and 23$^{\rm rd}$ April 2018. It was because of bad tracking during observations.

Then, the Shapiro-Wilk test of normality was applied. That test has the best power for a given sig-

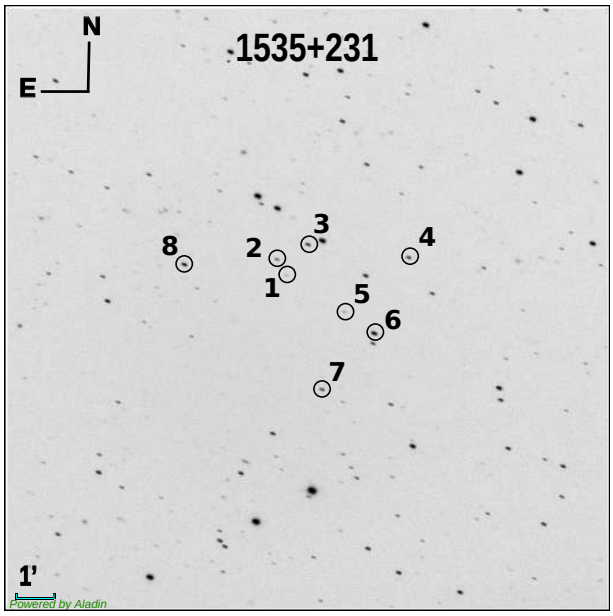

Fig. 1. *Chart of field of 1535+231.*

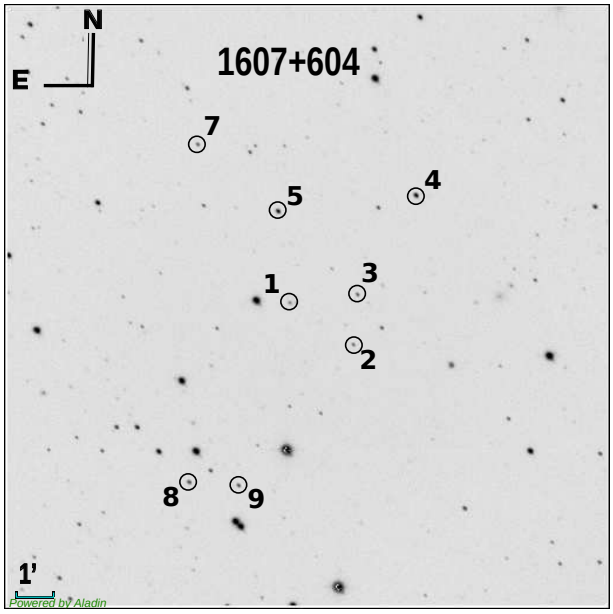

Fig. 3. *Chart of field of 1607+604.*

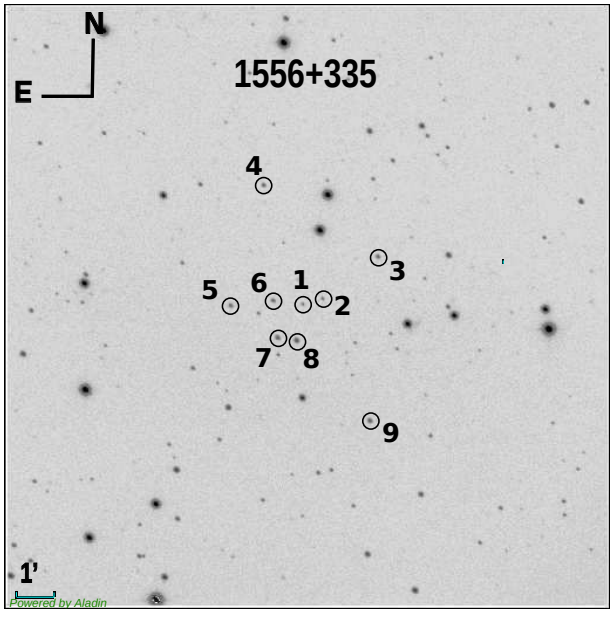

Fig. 2. *Chart of field of 1556+335.*

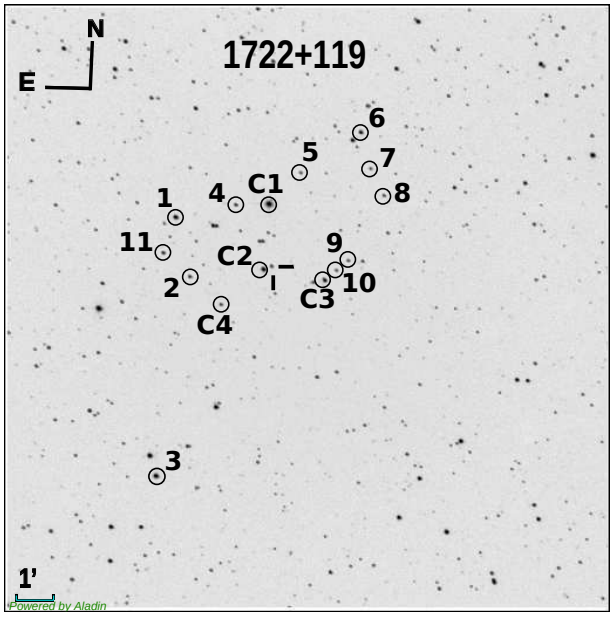

Fig. 4. *Chart of field of 1722+119.*

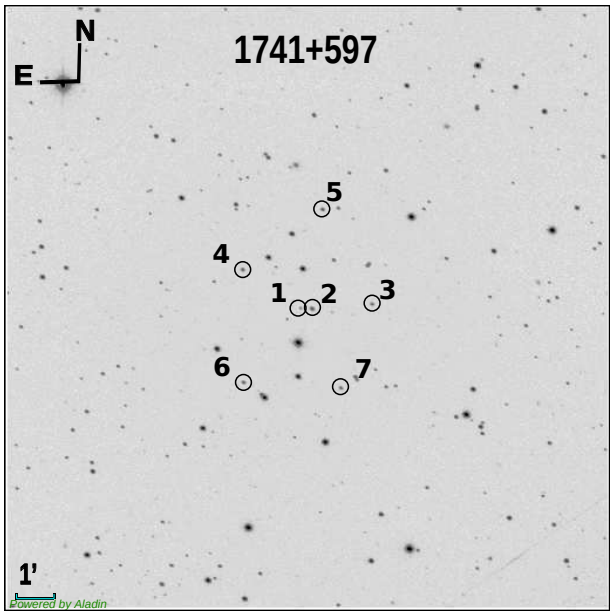

Fig. 5. *Chart of the field of 1741+597.*

nificance (Razali and Wah 2011), and it is restricted for sample size of less than 50 (as presented objects). After that, it is concluded that tests which require normal data distribution can be applied.

4.1. F–test

The F–test was used to determine the existence of brightness variability of objects and control stars (de Diego 2010, Gupta et al. 2017). We investigate variances of two (normally distributed) data sets to check are they equal to each other. The tested hypotheses are:

1) H_1: $\mathrm{Var}(O-A) = \mathrm{Var}(O-B)$
   H_{a1}: $Var(O-A) > Var(O-B)$ alternative,

2) H_2: $\mathrm{Var}(O-A) = \mathrm{Var}(A-B)$
   H_{a2}: $Var(O-A) > Var(A-B)$ alternative,

3) H_3: $\mathrm{Var}(O-B) = \mathrm{Var}(A-B)$
   H_{a3}: $\mathrm{Var}(O-B) > \mathrm{Var}(A-B)$, alternative.

Test statistics which correspond to these hypotheses are:

$$F_1 = \frac{\mathrm{Var}(O-A)}{\mathrm{Var}(O-B)},$$

$$F_2 = \frac{\mathrm{Var}(O-A)}{\mathrm{Var}(A-B)}, \text{ and}$$

$$F_3 = \frac{\mathrm{Var}(O-B)}{\mathrm{Var}(A-B)}.$$

Designations $O-A$, $O-B$, and $A-B$ refer to differences of obtained magnitudes of object and comparison star A, object and comparison star B, and comparison star A and B, respectively. The variances of mentioned differences are: $\mathrm{Var}(O-A)$,

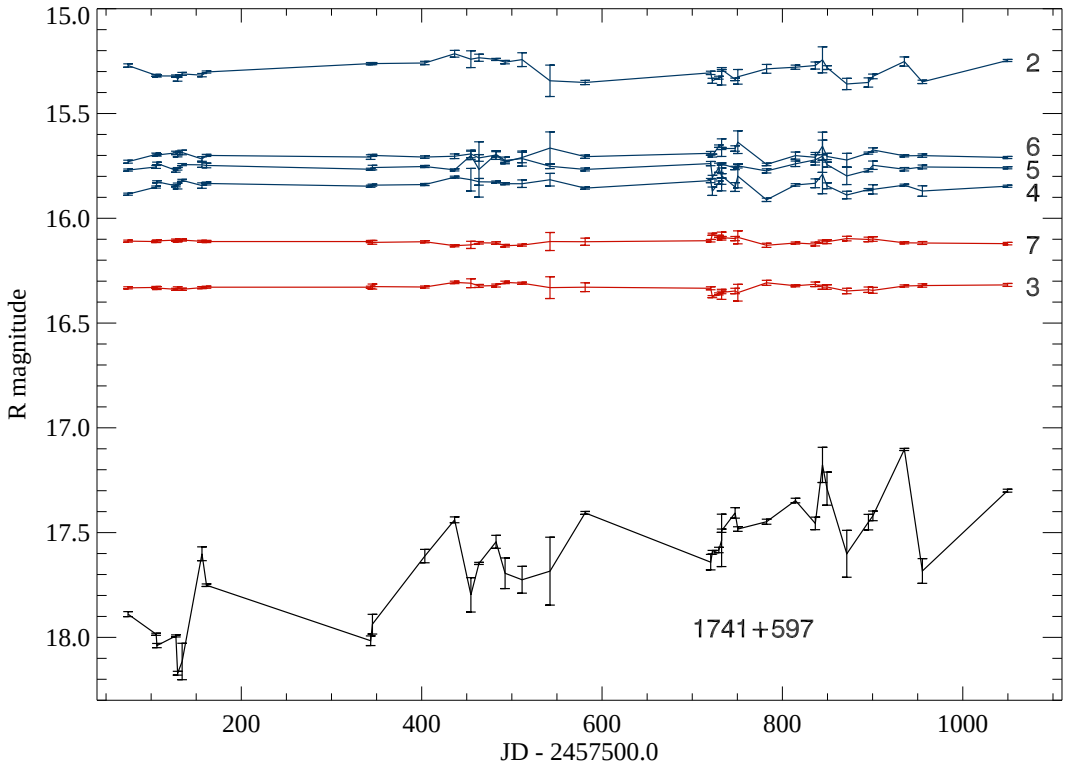

Fig. 6. *The light curves 1741+597 and its comparison and control stars from July 2016 until April 2019.*

$\mathrm{Var}(O-B)$, and $\mathrm{Var}(A-B)$. In the case of control star, O refer to its magnitude.

The F_i (i =1, 2, 3) values were compared with the critical value $F_c = F_n^{\alpha}$, where α is the significance level set for the test, and n signifies the number of degree of freedom equal to $N-1$, where N is the number of points.

The F–test was carried out for α values 0.05, 0.01 and 0.001 (correspond to probability of 95%, 99%, and 99.9% for acceptance of hypothesis), which roughly correspond to 2σ, 2.6σ and 3σ of sampling distribution, respectively. When the F_i value is greater than the critical, the null hypotheses H_i are discarded. For all objects it is expected that variances of mentioned differences ($\mathrm{Var}(O-A)$ and $\mathrm{Var}(O-B)$) should be close to each other. It means, F_1 value should be around 1, regardless of the brightness of object is stable or variable over time. If the brightness is changeable it should be in the same manner for both comparison stars, because they are stable a priori. The object is considered as variable if F_2 and F_3 are greater than the critical value F_c which corresponds to the significance level of 0.05. A similar investigation was done for each control star, just to put in the test suitable values for that star instead for the object.

4.2. Method of Least Squares

If there is some quasiperiodicity in the data set, the method of Least Squares (LS) could be used for sinusoidal parameters estimations (amplitude and phase) in line with suitable period:

$$f(t) = A\sin(\omega t + \varphi) + f_0, \tag{5}$$

where A is amplitude (in magnitudes), φ phase (in radians), ω angular velocity (in radians per days), and f_0 intercept (in magnitudes). Time t (in days) is the epoch of observation.

Eq. 5 can be expanded as follows:

$$\begin{aligned} f(t) &= A\cos(\varphi)\sin(\omega t) + A\sin(\varphi)\cos(\omega t) + f_0 \quad (6)\\ &= a_0 x_0 + a_1 x_1 + a_2, \quad (7)\end{aligned}$$

where $a_0 = A\cos(\varphi)$, $a_1 = A\sin(\varphi)$, $a_2 = f_0$, $x_0 = \sin(\omega t)$ and $x_1 = \cos(\omega t)$.

Coefficients a_i ($i = 0, 1, 2$) are estimated using LS three-parameter fitting method. Since ω is also unknown, the coefficients were estimated for a given set of periods P_j ($\omega_j = \frac{2\pi}{P_j}$). The minimum and maximum of P_j are about 0.3 years (in agreement with the Nyquist frequency) and 10 years (2.5 years is quarter of 10 years), respectively; the step is 0.1 years, observational period is 2.5 years.

The standard error of the estimate is $\sigma_0 = \sqrt{\frac{\sum (Y-f)^2}{N-3}}$, where f are LS fitting values, Y are data, and N is the number of data. Final coefficients a_i ($i = 0, 1, 2$) are determined for period P for which σ_0 has a minimum. If there are several local minimums, the procedure was repeated for each of them. Each sinusoidal solution was analysed. The amplitude and phase were calculated using equations:

$A = \sqrt{a_0^2 + a_1^2}$,
$\varphi = \arctan(a_1/a_0)$.

To detect systematic errors in residuals $(Y-f)_k$, $k = 1, ..., N$, Abbe's criterion was used according to Djurović (1979), Malkin (2013).

5. RESULTS

In order to investigate the presence of brightness variability of presented objects, we have followed the statistical analysis technique described in Subsection 4.1. As a result, the variability was detected for the four of five objects, in both filters. Three of the variable objects are BL Lac objects, and one is type QSO. The non-variable one (1556+335, QSO) has F_i (i =1, 2, 3) values almost equal to 1: F_1 =1.06, F_2 =1.06, F_3 =1.12 in V filter, and F_1 =1.54, F_2 =1.42, F_3 =1.08 in R filter. The critical value is F_c =2.33 for N =17 in V, and F_c =2.01 for N =24 in R; the significance level α =0.05.

In the case of variable objects, F_1 is around 1 as it is expected, but F_2 and F_3 are greater than critical value. The biggest F_2 and F_3 values are for objects 1722+119 and 1741+597 with large brightness variability.

For four variable objects, F_2, F_3, number of data points N, and critical values F_c (for N and $\alpha = 0.05$) are listed in Table 5 for both filters.

Table 5. The F–test results.

Object	Filter	N	F_2, F_3	F_c
1535+231	V	17	16.75, 20.91	2.33
	R	21	8.45, 11.56	2.12
1607+604	V	20	6.45, 7.34	2.17
	R	24	6.39, 6.48	2.01
1722+119	V	21	122.08, 113.93	2.12
	R	23	535.26, 547.43	2.05
1741+597	V	31	58.38, 59.96	1.84
	R	37	81.02, 81.29	1.74

In the case of control stars test shows that they are non variable.

For these objects, the method of LS was used to determine some periods in their brightness variability. Almost all objects have local minimum of σ_0 for periods around 0.5 years and 1 years. The presence of these periods is probably observational artifact (Rani 2009). Since this is an artifact, the annual variation was subtracted from our data, but the semiannual is not because of small amplitude. Calculated amplitudes for P = 1 year for objects 1535+231, 1607+604, and 1741+597 are in range from 0.056 mag to 0.174 mag. The 1722+119 has remarkable amplitude in both filters: 0.285 mag in V, and 0.322 mag in R filter. After that, the LS method was repeated on the residuals, and results of four variable objects (amplitude (A) and phase (φ)) are presented in Table 6 together with suitable periods (P), standard errors σ_0. The phase is referred

to epoch J2000.0. For some objects, in one filter quasiperiods are slightly different from the other filter because of different number N of input points. Also, more data in the future is going to give us more precise results. An example of LS fit on residuals (without annual variation) of R magnitudes for 1741+597 is in Fig. 7. The obtained quasiperiods are with 1.3 and 4.0 years. After removing these two sinusoids, the final residuals are presented in the same figure (below).

The final residuals (quasiperiods are removed, also) were examined using Abbe's criterion for significance level set: 0.05, 0.01, and 0.001. Abbe statistic $\gamma(N)$ was calculated as described in Djurović (1979) and Malkin (2013). For all objects $\gamma(N)$ was greater than the critical value $\gamma_0(N)$ for significance level $\alpha = 0.05$. The hypothesis that there is no trend in residuals can be accepted, and it is concluded that residuals could be explained with random variations. As example, for object 1741+597 (with $N = 37$ points in R) the value $\gamma(N) = 0.980$ is greater than critical value $\gamma_0(N) = 0.736$ for significance level $\alpha = 0.05$.

6. CONCLUSIONS

The monitoring data of five objects (3 BL Lac and 2 QSOs) in V and R magnitudes during the period of about 2,5 years are presented. The F–test is applied to test systematic variability. For four objects with systematic brightness variability the amplitude and phase of sinusoidal curve are estimated

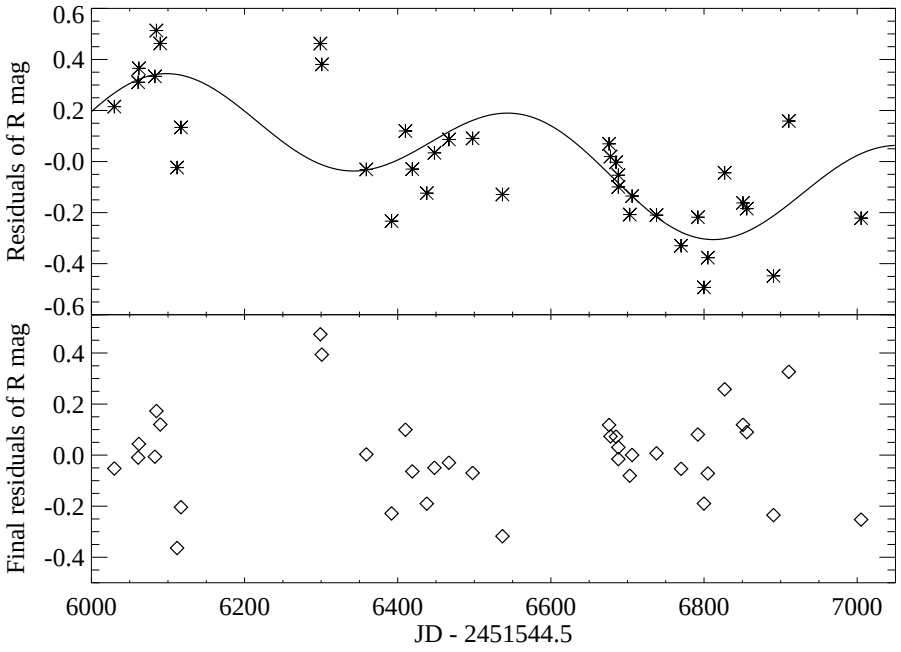

Fig. 7. *The LS fit of the light curve of 1741+597 in R band, and final residuals.*

Table 6. The amplitudes and phases (for the epoch J2000.0) of obtained quasiperiods for 1535+231, 1607+604, 1722+119, and 1741+597.

Object	Filter	σ_0 (mag)	$A \pm \sigma_A$ (mag)	$\varphi \pm \sigma_\varphi$ (°), J2000.0	P (yr)
1535+231	V	±0.08	0.16 ±0.02	57.1 ±10.3	3.1
	R	±0.13, ±0.10	0.19 ±0.03, 0.13 ±0.02	90.0 ±12.2, 181.2 ±13.0	1.7, 5.2
1607+604	V	±0.06	0.11 ±0.01	344.8 ±10.3	2.7
	R	±0.07, ±0.05	0.04 ±0.01, 0.09 ±0.01	173.2 ±31.0, 299.4 ± 9.1	1.3, 2.3
1722+119	V	±0.17, ±0.15	0.14 ±0.04, 0.12 ±0.03	184.9 ±22.0, 51.9 ±22.7	1.3, 2.7
	R	±0.17, ±0.14	0.12 ±0.03, 0.19 ±0.03	246.8 ±23.9, 176.9 ±12.0	1.3, 5.3
1741+597	V	±0.15	0.33 ±0.03	288.1 ±6.8	6.5
	R	±0.23, ±0.20	0.18 ±0.04, 0.16 ±0.03	152.2 ±16.9, 7.2 ±15.9	1.3, 4.0

using the method of LS. For almost all described objects there is brightness variability with annual period, and it is an observational artifact; only for 1722+119 it could be the real variability with amplitude about 0.3 mag in both bands. Quasiperiodic variations are presented in Table 6 for objects: 1535+231, 1607+604, 1722+119, and 1741+597. Their periods are from 1.3 to 6.5 years. In both filters some of them are with nearly the same value: 2.7 years in V and 2.3 years in R for 1607+604, and 1.3 years in both filters for 1722+119. Different periods in both bands for the same object could be because of different numbers of points in these filters. During our observational period July 2016 – April 2019, 1556+335 did not show brightness variability.

Calculated V and R magnitudes (see Table 3, input values) of all comparison and control stars are in a good agreement with observed ones (see Table 4, output values), in line with their standard errors. After implementing F–test and other tests, the significant brightness variability of these stars is not presented, and they are suitable for photometric measurements.

To investigate quasiperiods less than 0.3 years it is necessary to observe objects more frequently within a year, and to proceed observations in the case of quasiperiods greater than several years.

Acknowledgements – The author would like to thank her mentor Dr Goran Damljanović for guidance and support during this project. During the work on this paper the author was financially supported by the Ministry of Education, Science and Technological Development of the Republic of Serbia through the project 176011 "Dynamics and kinematics of celestial bodies and systems".

Funding for the Sloan Digital Sky Survey IV has been provided by the Alfred P. Sloan Foundation, the U.S. Department of Energy Office of Science, and the Participating Institutions. SDSS-IV acknowledges support and resources from the Center for High-Performance Computing at the University of Utah. The SDSS web site is www.sdss.org.

SDSS-IV is managed by the Astrophysical Research Consortium for the Participating Institutions of the SDSS Collaboration including the Brazilian Participation Group, the Carnegie Institution for Science, Carnegie Mellon University, the Chilean Participation Group, the French Participation Group, Harvard-Smithsonian Center for Astrophysics, Instituto de Astrofísica de Canarias, The Johns Hopkins University, Kavli Institute for the Physics and Mathematics of the Universe (IPMU) / University of Tokyo, the Korean Participation Group, Lawrence Berkeley National Laboratory, Leibniz Institut für Astrophysik Potsdam (AIP), Max-Planck-Institut für Astronomie (MPIA Heidelberg), Max-Planck-Institut für Astrophysik (MPA Garching), Max-Planck-Institut für Extraterrestrische Physik (MPE), National Astronomical Observatories of China, New Mexico State University, New York University, University of Notre Dame, Observatário Nacional / MCTI, The Ohio State University, Pennsylvania State University, Shanghai Astronomical Observatory, United Kingdom Participation Group, Universidad Nacional Autónoma de México, University of Arizona, University of Colorado Boulder, University of Oxford, University of Portsmouth, University of Utah, University of Virginia, University of Washington, University of Wisconsin, Vanderbilt University, and Yale University.

REFERENCES

Abolfathi, B., Aguado, D. S., Aguilar, G. et al.: 2018, *Astrophys. J. Suppl. Ser.*, **235**, 42.

Bourda, G., Collioud, A., Charlot, P., Porcas, R. and Garrington, S.: 2011, *Astron. Astrophys.*, **526**, A102.

Chonis, T. S. and Gaskel, M. C.: 2008, *Astron. J.*, **135**, 264.

De Diego, J. A.: 2010, *Astron. J.*, **139**, 1269.

Djurović, D.: 1979, *Matematička obrada astronomskih posmatranja*, University of Belgrade (in Serbian).

Doroshenko, V. T., Efimov, Yu. S., Borman, G. A. and Pulatova, N. G.: 2014, *Astrophysics*, **57**, 176.

Fey, A. L., Gordon, D., Jacobs, C. S. et al.: 2015, *Astron. J.*, **150**, 58.

Gaia Collaboration, Mignard, F., Klioner, S. A., Lindegren, L. et al.: 2018, *Astron. Astrophys.*, **616**, A14.

Gupta, A. C.: 2014, *J. Astrophys. Astr.*, **35**, 307.

Gupta, A. C., Agarwal, A., Mishra, A. et al.: 2017, *Mon. Not. R. Astron. Soc.*, **465**, 4423.

Malkin, Z. M.: 2013, *Astron. Rep.*, **57**, 128.

Popović, L. Č., Jovanović, P., Stalevski, M. et al: 2012, *Astron. Astrophys.*, **538**, A107.

Rani, B., Wiita, P. J. and Gupta, A. C.: 2009, *Astron. J.*, **696**, 2170.

Razali, N. M. and Wah, Y. B.: 2011, *Journal of Statistical Modeling and Analytics*, **2**, 21.

Taris, F., Souchay, J., Andrei, A. H. et al.: 2011, *Astron. Astrophys.*, **526**, A25.

Taris, F., Andrei, A., Roland, J. et al.: 2016, *Astron. Astrophys.*, **587**, A112.

Taris, F., Damljanovic, G., Andrei, A. et al.: 2018, *Astron. Astrophys.*, **611**, A52.

Tody, D.: 1986, in Proceedings SPIE Instrumentation in Astronomy VI, ed. D.L. Crawford, **627**, 733

Tody, D.: 1993, in Astronomical Data Analysis Software and Systems II, A.S.P. Conference Ser., eds. R.J. Hanisch, R.J.V. Brissenden, & J. Barnes, **52**, 173

ИСПИТИВАЊЕ ПРОМЕНЕ СЈАЈА НЕКИХ КВАЗАРА ВАЖНИХ ЗА ПОВЕЗИВАЊЕ ICRF – GAIA CRF

M. D. Jovanović

Astronomical Observatory, Volgina 7, 11060 Belgrade 38, Serbia
E–mail: *miljana@aob.rs*

УДК 524.7 : 521.96 ICRF, Gaia CRF
Оригинални научни рад

У овом раду су представљени фотометријски подаци за пет објеката (1535+231, 1556+335, 1607+604, 1722+119 и 1741+597) и њихових 30 упоришних звезда посматраних у V и R филтерима. Они чине узорак од 47 објеката погодних за повезивање ICRF и Gaia CRF. Коришћена су три телескопа: два се налазе на Астрономској станици Видојевица (60 cm и 1.4 m) и један на опсерваторији Рожен у Бугарској (2 m). Редукција снимака је урађена коришћењем софтверског пакета Iraf, док је сјај објеката израчунат диференцијалном фотометријом у софтверу MaxIm DL. Промена сјаја објеката у посматрачком периоду од јула 2016. године до априла 2019. године је испитана F-тестом, и за 4 варијабилна објекта одређен је период у промени сјаја у оба филтера методом најмањих квадрата. За објекат 1535+231 израчунат је период од 3.1 године у промени сјаја у V, а 1.7 и 5.2 године у R филтеру, за 1607+604, 2.7 година у V и 1.3 и 2.3 година у R филтеру, за 1722+119, 1.3 и 2.7 година и 1.3 и 5.3 година и 1741+597, 6.5 година и 1.3 и 4.0 година. Само се објекат 1556+335 у овом периоду показао као стабилан. На исти начин је одређен сјај упоришних звезда ових објеката. Након испитивања промена њиховог сјаја, може се закључити да све звезде (укупно 30) могу да буду коришћене за диференцијалну фотометрију. Дате су њихове координате, магнитуде и графици на којима су означени објекти и звезде.